Article can be accessed online at http://www.publishingindia.com

An Adaptive Fusion of Noisy Images for Multi Modal Medical Image Application

Marappan Shanmugasundaram*, S. Sukumaran**

Abstract

Multimodal medical images lends to certain problems in the medical imaging fusion system, since the devices introduces noise during the process of image capturing. Because of the appearance of noises in the input images, it leads to trouble as introducing artifacts in the resulted image of fusing the degraded images. This paper proposes a fusion approach for noisy images, captured from two different modalities, that merge adaptively unique details of the images denoised by i) bilateral method ii) curvelet method iii) 2D modulated filter bank method. For the fusion of denoised images, weight may be calculated by residuals of the recommended filtering methods. Performance measures required to show the stability of the proposed method are effectively employed in comparing the results with other state-of-the-art fusion methods.

Keywords: Fusion, Residual, Bilateral, Curvelet, Denoise, Filter Bank

1. Introduction

The purpose of image fusion is to merge more than one image of the same scene into a single image that holds important features of the source images [1]. The outcome of the fused image seems to be fit for further relevant process including segmentation, feature extraction, object identification and classification. With the quick improvements in the development of multiple image sensors, different image decomposition techniques have been developed to acquire various spectral and spatial details from the image [2]. So the rapid growth of the fusion technology is determined by the help of multi-sensor and image decomposition, that facilitates the beneficial effects in a number of areas such as modern military, medical and civilian imaging applications[3][4]. But, the utilization of sensors in spectral fusion results information overloads because of data redundancy [5]. Hence multiresolution image fusion shall be an efficient mechanism to overcome the limitations [6].

Medical image analysis is a process in diagnosis and clinical investigation to maintain the history of a patient to provide better treatment. Generally, images captured by medical sensors contain various noises [7] that affect the expert's decision-making from taking necessary actions in the diagnosis. Even an experienced physician may struggle in taking his valuable diagnosis procedure and opinion when the images are not properly preprocessed. Therefore, the quality of these images has to be enhanced without contaminating the important features for preserving some significant geometrical structures. On the other hand, several proposals have been developed to denoise medical images in the literature. Some of the methods include wavelet transform [8][9], Total Variation [10] and adaptive filters [11][12] have been used for this purpose. Recently, image fusion is one of the most popular methods in denoising medical image that shows an incredible performance by combining multimodality information into a single image. Fused image helps efficient diagnosis by giving best results with high accuracy and reliability of multi sensor medical images [4]. For example, the fusion of MRI and CT images offer the details of soft tissue and bone where MRI contributes soft tissue and CT contributes bone information. Popular medical image fusion is employed on brain imaging in

* Ph.D Research Scholar, Department of Computer Science, Erode Arts and Science College, Erode, Tamil Nadu, India.
E-mail: shanmugapriyansp@gmail.com

** Associate Professor, Department of Computer Science, Erode Arts and Science College, Erode, Tamil Nadu, India.
E-mail: prof_sukumar@yahoo.co.in

finding the root cause of stroke, intracranial haemorrhage, trauma, skull fracture, oncology, neurological problems etc. CT and MRI images are influenced by Additive Gaussian noise [12][13].

Recently, the residuals acquired by subtracting the denoised image from noisy image has attracted a great interest in providing useful knowledge about the noise and foreground details of the natural image. So, to retrieve fine edges and textures, more attention is required to separate foreground details from the residuals. In the literature, most of the algorithms used to fuse medical images leads to a serious problem because of the noise existed in the source images. Moreover, the significant details required for feature identification are lost in preprocessing. This prompts us to generate a novel fusion algorithm to use the beneficial residuals concerning with fusion for multimodality noisy images. In related to this, in [14], to obtain fine edges and textures from noisy image, the residuals derived from denoising the noisy CT and MRI images using curvelet and TV methods are respectively denoised by curvelet transform. To show the ability of increasing high entropy in the fused image, the extracted details from the residuals are fused with the denoised images. Similarly, Angelini et al.[15] proposed a fusion system, which gives PET and SPECT image fusion based on brushlet that suits for enhancement of textures and cubic spline function suited for enhancement of contours. Furthermore, a coefficient module map is used for calculating threshold based fusion rule for the final fused image.

From the literature, it is found that, bilateral filter proved its best performance for preserving edges during noise removal from the noisy image but it fails in preserving textures and curves [16][17]. However Curvelet is the best choice in serving long and curve edges but it introduces pseudo-Gibbs-artifacts in the homogeneous area [18][19]. On the other side, 2D Modulated Filter bank [20] have shown its best performance in acquiring textures, but the filtered image is influenced by artifacts in boundaries and smooth area during the process of denoising. Based on this study, this paper presents a novel fusion approach for medical CT and MRI noisy images and the procedure is as follows : The source noisy images are i) denoised by bilateral method ii) denoised by curvelet method iii) denoised by 2D modulated filter bank method, where fusion weight is calculated by the residuals of the recommended methods.

This organization of this paper follows as: Section 2 gives a brief description and usage about bilateral filter. Curvelet and its mathematical derivations are described in section 3. In section 4, the functionality of 2D modulated filter bank is discussed. The proposed method is expressed in section 5. In section 6, results obtained from the suggested method and comparisons are experimented. Finally, section 7 presents the conclusions of this paper.

2. Bilateral Filter

Bilateral filtering provides an efficient direction to smoothing an image while protecting its discontinuities. It presents a beneficial path to distilling image-structures of different scales [16]. Smoothing may be achieved by calculating a weighted average of neighboring pixels through convolution in both spatial and range domains [21]. Basically it is derived from the combination of Gaussian low-pass filter and an edge stop function. So, the combination of these both would result a denoised image with preserving edges. To determine the weights of a pixel, it doesn't only depend on nearby pixel locations but also on pixel range values.

At the time of smoothing an image, consider x to be the centre pixel that can be replaced a bilateral filter as:

$$F_x = \frac{1}{n(x)} \sum_{x^1 \in \Omega} g_s\left(\left\|x^1 - x\right\|\right) g_r\left(I_p - I_{p^1}\right) I_{p^1} \tag{1}$$

Where x^1 represents neighborhood pixel and the term norm illustrates the Euclidean distance from the centre pixel to its nearby pixels. This setup is expressed as spatial domain and is denoted by g_s in eqn. (1). In the second part of the eqn. (1), I_p constitutes the intensity value of the centre pixel and I_{p1} acts as the intensity value of the neighborhood pixel. This arrangement is demonstrated in terms of range domain and is denoted as g_r. Finally, n(x) is normalization factor and is exposed as:

$$n(x) = \sum_{x^1 \in \Omega} g_s\left(\left\|x^1 - x\right\|\right) g_r\left(I_p - I_{p^1}\right) \tag{2}$$

In the above expression, the distance between the pixels is fixed for computing weighted by the function g_s in spatial domain, and the function g_r fixes the weight in the range domain. The image quality obtained by bilateral filtering is specified by domain and range parameters. In order to fluctuating the values of the parameters, different kind of responses such as cartoon and residual may be obtained with various spatial and spectral details. In this way,

increasing the value of the parameter domain provides cartoon as images on the other hand increasing range value results blurring the images.

Smoothing the images iteratively using bilateral filter produces more spectral information of input image. The process of iteration makes the result almost piecewise invariant. Even though the bilateral filter results smoother images repeatedly, they are not similar when enhancing the spatial and range arguments. The cause of enhancing spatial argument depends on the range argument. Unless either parameter is increased or decreased the rest cannot be affected.

To measure and calculate noise model of the image, noisy image can be separated. During this process, a most knowledgeable residual image can be derived by performing a subtraction between noisy and filtered images. It is possible to make use of the residuals in terms of estimating and constructing a noise model for retrieving fine details.

3. Curvelet Transform

CT (Curvelet transform) is one of the popular multiscale mechanisms, possessing a right nature of directional information which yields a rich anisotropic at fine scales [22]. To construct curvlets, a multiscale ridgelet is combined with bandpass filters in this system. The curvy details that are the most important feature of the signal can be preserved by a parabolic scaling law: $width \cup length^2$ [22] [19], achieved through fixing a set of band pass filters. Apart from ridgelet, it utilizes wavelet to obscure the signal at several scales and each scale is partitioned into small regions. Big regions are employed to divide the big scale wavelet components plus small regions are applied to divide the small wavelet components. Ultimately, each region is demanded by ridgelet transform to retrieve the edges at a particular scale. The notion behind this is the edges contained in each scale are almost like straight lines. Inadequately curvelet occurs in all positions and orientations.

Transparently a signal would break up into different scales in multiscale transformation. Each scale presents different knowledge about the signal. A group of low-pass and band-pass filters can be accomplished to break up the signal into various scales. Different frequencies are placed for each one.

$$f \to (p_o f, \Delta_1 f, \Delta_3 f, ...) \tag{3}$$

where p_o and Δ carries low pass filter and a series of high pass filters. Energy preservation is defined by the following function.

$$f = p_o(p_o f) + \Sigma\Delta_s(\Delta_s f) \tag{4}$$

The recursive construction field is constructed by:

$$\Psi_{2s}(s) = 2^{4s}\Psi\left(2^{2s}X\right) \tag{5}$$

The approximation coefficients of wavelet transform are obtained by applying convolution over sub-bands obtained in the former step. The input signal f is broken up into S_o, D_1, D_2, D_3.

$$p_o f = \phi_o \times f \qquad \Delta_s f = \Psi_{2s} \times f \tag{6}$$

The input image for curvelet transform is decomposed as sub bands from the above series of procedure. Each subband is involved into the smoothing by a window with the size of $2^5 \times 2^{-2}$.

$$h_Q = W_Q . \Delta_s f \tag{7}$$

where, W_Q gives a group of smooth windowing functions. A set of dyadic squares Q_s is generated at scale s is dyadic function and each dyadic square is computed by:

$$Q_{s,k_1,k2} = \left[\frac{k_1}{2}, \frac{k_1+1}{2}\right] \times \left[\frac{k_1}{2^s}, \frac{k_2+1}{2^s}\right] \in Q_s \tag{8}$$

Eqn. (7) and (8) denotes the process of smooth partitioning.

In the next step, each dyadic square must be renormalized to the unit square $[0,1]\times[0,1]$

$$g_Q = T_Q^{-1} h_Q \tag{9}$$

where T_Q - normalization operator , Q - dyadic square is formulated as:

$$\left(T_Q f\right)(x_1, x_2) = 2^s f\left(2^s x_1 - k_1, 2^s x_2 - k_2\right) \tag{10}$$

Eqn. (9) and (10) contributes in renormalization operation.

After normalizing the square, it can have the details of line, curve and angle which are named as ridges. Those ridges can be decoded in the radon transform. In radon domain, usually ridges are built up as a wavelet.

The mathematical representation of radon transforms and it is defined as:

$$Rf(\theta,t)=\int f(x_1,x_2)\delta(x_1\cos\theta+x_2\sin\theta-t)\,dxdy \quad (11)$$

Generally ridgelet transform is the best result of one dimensional wavelet transform. So it shares the primary features of wavelets that assist to discover the curve angle and location. Ridgelet element in the frequency domain is computed by:

$$\hat{\rho}_\lambda(\xi)=\frac{1}{2}|\xi|^{-\frac{1}{2}}\left(\hat{\psi}_{j,k}(|\xi|).\omega_{i,l}(\theta)+\hat{\psi}_{j,k}(-|\xi|).\omega_{i,j}(\theta+\pi)\right) \quad (12)$$

From eqn. (12), $\omega_{(i,j)}$ gives periodic wavelets in the interval of $[-\pi,\pi]$. i present the angular scale and $\psi_{(j,k)}$ develops a Meyer wavelet set. Ultimately j and k acquire scale and location of ridgelet.

4. 2D Modulated Filter Bank

2-D separable DFT modulated filter banks offer 2-D frequency tiling. Compare with other 2-D filter banks it is entirely different that they are yielded by the tensor of two 1-D separable DFT modulated filter banks [20]. It uses subband filters in order to select frequency direction. Based on its 2-D frequency feature, regions may be divided as solely or individually symmetric [23][24]. The 1-D separable modulated filter bank is defined as:

Say

$$F_n(\omega)=F\left(\omega-2\pi n/N\right),\quad n=-\left[(N-1)/2\right],...,0,1,...\left[N/2\right] \quad (13)$$

is an 1-D DFT modulated filter bank with M channel. Then, the 2-D separable oversampled NPR DFT modulated filter bank is defined as:

$$F_{n,k}(\omega_i,\omega_j)=F\left(\omega_i-2\pi n/N\right)F\left(\omega_j-2\pi k/N\right)$$
$$b_{n,k}(v_i,v_j)=b(v_i)b(v_j)e^{2\pi r(nv_i+kv_j)/N} \quad (14)$$
$$n,k=-\left[(N-1)/2\right],...,0,1,..\left[N/2\right]$$

To focus more attention on texture details, the same 1D DFT filter bank can be employed in horizontal and vertical directions. In fact, the horizontal and vertical directions can also use different 1-D DFT filter banks. The filters in (14) use such a subscript arrange for that the subscripts can indicate the quadrant of the frequency supports of the subband filters. For example, when the subscripts m and k are positive integers, the frequency support of the subband filter would be in the first quadrant of the 2-D frequency plane.

5. Proposed Adaptive Fusion Algorithm

This section discusses the proposed fusion technique that applies bilateral, CT and 2D modulated Filter bank. The primary operations of these methods are meant for sparse and appreciable results in particular fields in an image. Bilateral filtering gives superior noise removal effects in the edge region in an image, but unable to recapture the textural areas in the right manner. CT based denoising rebuilds curve details on high quality but bring

Figure 1. Basic Structure of The Proposed Fusion System Using Residuals and Variance Map

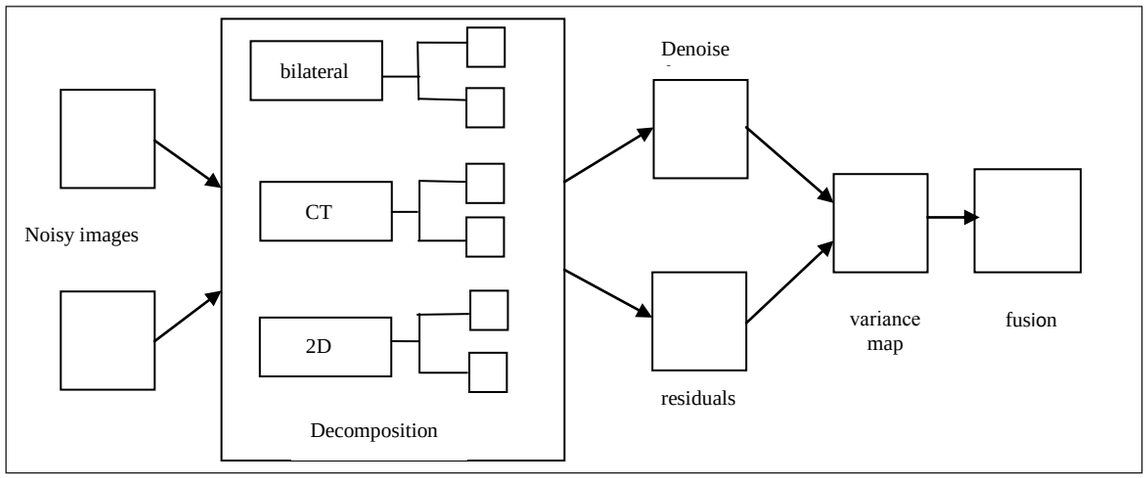

in pseudo-Gibbs-artifacts in flat areas. Textures can best be secured in 2D modulated filter bank, but side effect again would result in contour of objects and smooth areas. In the succeeding sections, the proposed fusion method is discussed briefly and the functionalities are illustrated in fig. 1.

5.1. Detection of Substantial (Significant) Features

For fused image, according to [14][25], detection of various significant features of the signal may be obtained by smoothing the signal with different filtering techniques. By this approach, unique details of the signal can be highlighted in resulted image.

In this paper, the source noisy images captured from the two different modalities are i) denoised by bilateral method ii) denoised by curvelet method iii) denoised by 2D modulated filter bank method respectively. However, the noise-free images obtained by bilateral filter represent smooth region and linear edges because of its most significant edge preserving features. In fact, the nature of maintaining curve information is possessed in the resulted noise free images since they are denoised by the robust CT. On the other hand, the textures superimposed by noises can possibly be separated in the resulted images because of the effective utilization of 2-D separable DFT modulated filter bank. The noise-free images are effectively demonstrated as if various local qualities exist in spatial domain.

5.2. Decomposition

For noisy images, it is decomposed into two components such as denoised and residual. According to [26], the model of this procedure is constructed by:

$$I_n = I_d + I_r \tag{15}$$

In the above model, the component I_d proposes the geometric information and is very close to smooth region and edges. The component I_r contains noise detail and is very near to textures extracted from noisy image. In this work, the decomposition of noisy image is made by three different filtering techniques as shown in sections 2-4. The residual is obtained from the model as:

$$I_r = I_n - I_d \tag{16}$$

In the proposed method, a group of residual models is constructed in terms of computing the difference between noise and smoothed images. Since the residual incorporates noise and less geometrical structure details, it serves as estimation of noise level as well as determination of weights, shown in section 5.4 , to be used for the fusion. The local quality of the denoised image is estimated by obtaining the deviation from the residual and denoised images. The residual and error models can be shown in fig 4.

5.3. Variance Map

A variance map consists of a collection of variances. Variance is computed for each pixel in the image. A specified size of window is required to measure variance for every pixel in the image. On the variance map, each centre pixel of the image is replaced by the variance under the specified mask. So, the window is traversed the entire image pixel by pixel. In this work, this procedure is employed to the groups of residual images which are obtained through computing the difference between noise and smoothed images. Since the residual incorporates noise and less geometrical structure details, it serves as estimation of noise level in denoising as well as determination of weights to be used for fusion. The local quality of the denoised image is estimated by obtaining the deviation from the residual and denoised images. Indeed, this would aim to retrieve the geometric definition from noisy data. So, the local variance is computed as:

$$\sigma_m(x,y) = \sum_{i=1}^{n} \left(p_i - \bar{p} \right)^2 / (n-1) \tag{17}$$

where (x,y) belongs to the mask with size of 3x3, and n indicates the number of elements under the mask, p represents mean value, p_i acts as centre pixel and m represents the number of variance maps. Obviously a set of variances would have to be measured based on the number of source images used to fuse. As per our problem, two sets of variances, each for one source, need to be computed. So, totally three variance maps have to be demanded for each source image.

5.4. Computing Fusion Weight

Simple pixel fusion done by averaging two denoised image does not provide better execution. The artifacts as forming

wrinkles in the homogeneous part and edge part would be survived in the denoised curvelet image which tends to be added in the fused image. Similarly adding two images ominously results high contrast in the fused image. So, we introduce a weighted scheme in terms of diminishing the high contrast and vanishing the artifacts in the final fused image. The detail required to perform weight is computed by generating deviation of the variance of residual image from the variance of a noisy image. Next, the weight, which needs to be computed by variances estimated in section 5.3 using the given formula:

$$w_m(x,y)=1-\frac{\left|\sigma_m(x,y)-\sigma^2\right|^{\alpha}}{\left|\sigma_1(x,y)-\sigma^2\right|^{\alpha}+\left|\sigma_2(x,y)-\sigma^2\right|^{\alpha}+\left|\sigma_3(x,y)-\sigma^2\right|^{\alpha}},m=1,2,3 \quad (18)$$

where α is a metric and $\alpha \geq 0$, σ^2 represents the variance of noisy image, σ_1, σ_2 and σ_3 constitutes variances of residuals of three proposed denoised methods. Based on these procedures, the residuals are getting preprocessed for receiving the geometrical structures.

5.5. Fusion of Denoised Images

In the field of pixel-level fusion, among the several fusion methods including multiresolution and multiscale, arithmetic fusion algorithms are not much complicated and provide effective fusion results. This kind of algorithms represents the resulted image pixel by pixel, as a combination of pixels in the corresponding locations of the source images. This procedure is represented as:

$$f(x,y)=w_a s_1(x,y)+w_b s_2(x,y)+c \quad (19)$$

where x and y constitute the pixel location, s_1, s_2 and f acts as a source and fused images respectively, w_a and w_b are constants that they are used to specify the direction to the individual sources for the fused image. C represents the mean offset and is constant.

The denoised images fused in the proposed methods are step in the fusion process based on the adaptive weighted average. Because, a simple addition of two images does not provide good results like artifacts in the homogeneous area, repetition of edges and textures. However, proper use of weight overcomes these problems. Consider s_1, s_2 and s_3 are denoised images by the proposed methods, w_1, w_2 and w_3 computed in section 5.4 are power determining the relative influence for the fused image. This procedure is described as:

$$f(x,y)=\left(w_1(x,y)s_1(x,y)+w_2(x,y)s_2(x,y)+w_3(x,y)s_3(x,y)\right) \quad (20)$$

where, f indicates the fused image in which a combination of three unique features derived from three different denoising techniques would be transferred. This fused image provides effectively best results in making qualitatively noise free as well as in retrieving full-fledged foreground information.

5.6. Final Image Fusion

By this way, the noisy input images seem to be denoised and unique features can adaptively shift to the intermediate images by using eqn. (20). Finally, a simple average based fusion can be applied over the intermediate images to acquire the complementary information.

$$f_{(p,q)}(x,y)=0.5*\left[F_1(x,y)+F_2(x,y)\right] \quad (21)$$
$$p,q=1,2,3,\ldots N$$

Shortly, the steps of the algorithm follow as:

Firstly, the source noisy images $A(x,y)$ and $B(x,y)$ captured from the two different modalities are i) denoised by bilateral method ii) denoised by curvelet method iii) denoised by 2D Filter bank method respectively. However, the noise-free images A_d^{BT} and B_d^{BT} are the representative bilateral filter. A_d^{CT} and B_d^{CT} images are denoised by the robust curvelet transform. At the same time, A_d^{2D} and B_d^{2D} are the instances of the effective utilization of 2-D separable DFT modulated filter bank. The noise-free images are effectively demonstrated as if various local qualities are exist in spatial domain. Secondly, groups of residual images are obtained as illustrated in section 5.2 and they are represented as A_r^{BT}, A_r^{CT}, A_r^{2D} for input A and B_r^{BT}, B_r^{CT}, and B_r^{2D} for input B. Thirdly, the deviation of local variance is computed. Fourthly, the weight, which needs to be computed by variances estimated in the former step using the formula given in eqn. (18). Next, the A-series denoised images are fused and results as an intermediate fused image $f_1(x,y)$. Similarly B-Series denoised images result $f_2(x,y)$ based on their local quality measure. Finally, a simple average fusion can be applied over the intermediate images to acquire the complementary information.

Input : noisy image A & B with size $M \times N$
Output: fused image F

// /smoothed images of input image A are A_d^{BT} , A_d^{CT} and A_d^{2D}

// /smoothed images of input image B are B_d^{BT} , B_d^{CT} and B_d^{2D}

for i=1 to M

for j= 1 to N

// / smoothed by bilateral

$$A_d^{BT}(i,j) \,\&\, B_d^{BT}(i,j) = \frac{1}{n(x)} \sum_{x^1 \in \Omega} g_s\left(\left\|x^1 - x\right\|\right) g_r\left(I_p - I_{p^1}\right) I_{p^1}$$

// /smoothed by curvelet

$$A_d^{CT}(i,j) \,\&\, B_d^{CT}(i,j) = \begin{cases} C^{coefficient}, & \left|C^{coefficient}\right| \geq k\ v_1 v_2 \\ o & otherwise \end{cases}$$

// /smoothed by 2D modulated filter bank

$$F_{n,k}(\omega_i, \omega_j) = F\left(\omega_i - 2\pi n / N\right) F\left(\omega_j - 2\pi k / N\right)$$

$$A_d^{2D}(i,j) \,\&\, B_d^{2D}(i,j) = b_{n,k}(v_i, v_j) = b(v_i) b(v_j) e^{2\pi r\left(n v_i + k v_j\right)/N}$$

$$n,k = -\left[(N-1)/2\right], \ldots, 0, 1, \ldots \left[N/2\right]$$

endfor

endfor

// creating residuals

for i=1 to M

for j= 1 to N

// residual od source A

$$A_r^{BT}(i,j) = A(i,j) - A_d^{BT}(i,j)$$

$$A_r^{CT}(i,j) = A(i,j) - A_d^{CT}(i,j)$$

$$A_r^{2D}(i,j) = A(i,j) - A_d^{2D}(i,j)$$

// residuals of source B

$$B_r^{BT}(i,j) = B(i,j) - B_d^{BT}(i,j)$$

$$B_r^{CT}(i,j) = B(i,j) - B_d^{CT}(i,j)$$

$$B_r^{2D}(i,j) = B(i,j) - B_d^{2D}(i,j)$$

endfor

endfor

//for all residuals

for i=1 to M

for j= 1 to N

$$\sigma_m(i,j) = \sum_{i=1}^{n} \left(p_i - \bar{p}\right)^2 / (n-1)$$

$$w_m(i,j) = 1 - \frac{\left|\sigma_m(i,j) - \sigma^2\right|^\alpha}{\left|\sigma_1(i,j) - \sigma^2\right|^\alpha + \left|\sigma_2(i,j) - \sigma^2\right|^\alpha + \left|\sigma_3(i,j) - \sigma^2\right|^\alpha}, m = 1,2,3$$

endfor

endfor

//intermediate and final fusion

for i=1 to M

for j= 1 to N

$$f_1(i,j) = \begin{pmatrix} W_1(i,j) * A_1(i,j) + W_2(i,j) * \\ A_2(i,j) + W_3(i,j) * A_3(i,j) \end{pmatrix}$$

$$f_2(i,j) = \begin{pmatrix} W_1(i,j) * B_1(i,j) + W_2(i,j) * \\ B_2(i,j) + W_3(i,j) * B_3(i,j) \end{pmatrix}$$

$$f(i,j) = 0.5 * \left[f_1(i,j) + f_2(i,j)\right]$$

endfor

endfor

Figure 2. Pseudo Code of the Proposed Fusion Technique

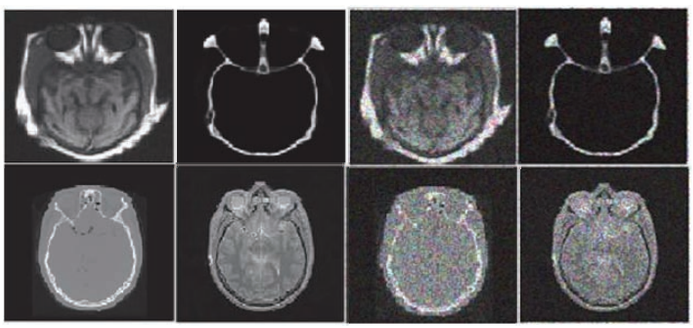

6. Results and Discussions

The proposed algorithm has been implemented in MATLAB 7 and examined on two pair of medical images. To show the strong influence on the fusion of the proposed method, the source images are contaminated by adding multiplicative noise distributed randomly with 0 mean and 0.04 variance. Totally six different parameters

and three state-of-the-art fusion methods are used in evaluating the algorithm. The parameters such as entropy, standard deviation and fusion symmetry [25] have been calculated in order to estimate the quality of fusion. On the other hand, another three more parameters including VIF (visual information fidelity), MI (mutual information) and Q_{AB}^{F} are utilized to expose the evidence of the benefits to denote edge and texture details. MI present the amount of mutual information shifted from source images to a fused image based on information theory [27]. VIF judges the quality of fused images in terms of the human visual system, distortion of signal and natural scenes [28].

Edge strength:

The edge details provided by fusing image are estimated by this parameter and it is visually supported by the human visual system. With this approach, the strength of the edge and orientation can be achieved by Sobel operator.

$$Q_{AB}^{F} = \frac{\sum_{i=1}^{N}\sum_{j=1}^{M} Q^{AF}(n,m)W^{A}(n,m)Q^{BF}(n,m)W^{B}(n,m)}{\sum_{i=1}^{N}\sum_{j=1}^{M} W^{A}(i,j)+W^{B}(i,j)} \quad (23)$$

The edge preservation measures for input image A and B are $Q^{AF}(n,m)$ and $Q^{BF}(n,m)$ that contributes along with its weight W^{A} and W^{B} to calculate the strength of edges exists toward the inside of the image.

Standard deviation:

It is another parameter to estimate the quality of the fused image $M \times N$ by the given formula:

$$\sigma = \sqrt{\frac{1}{MN}\sum_{m=1}^{M}\sum_{n=1}^{N}(f(n,m)-\mu)^{2}} \quad (24)$$

$f(n,m)$ - pixel value in the location; μ - averages of pixels. If the fused image results high standard deviation value then the fused quality is improved.

Entropy:

The parameter entropy judges the amount of details transferred from source images to fused one. In another way it provides the amount of information content contained in the fused image. Logically the high value fused one can have large details than lower value. Entropy is defined as

$$E = -\sum_{l=0}^{L-1} P_l \log_2 P_l \quad (25)$$

where L – number of intensity level; l – intensity value; P_i - proportion between overall pixels of l and number of overall pixels.

Fusion symmetry:

It is estimated the symmetry of mutual information for fused image and represent

$$FS = abs\left(\frac{I_{AF}}{I_{AF}+I_{BF}} - 0.5\right) \quad (26)$$

I_{AF} - A common data between source image A and fused image F

I_{BF} - A common data between source image B and fused image F

In order to show the effective performance of the proposed method, it is compared with some multiresolution and multiscale image fusion methods including DWT, CT and NSCT. For removal of noise in the wavelet domain, a bior (2, 2) filter which is originated by biorthogonal wavelet is used. For the same purpose, the pyrexc filter is employed in NSCT based denoising. The above filtering mechanism shows the supreme performance for the above methods [29]. In curvelet domain, hard thresholding method for removing noise in the corrupted image has been proposed [19]. The basic principle of hard thresholding used in the curvelet transform for denoising a signal is similar to wavelet transform. In this approach, the threshold value is determined by variances of noise image and the curvelet coefficient. For all comparison methods, the pixel-level average has been adopted in fusing the sources.

According to bilateral filter, the parameters include the size of the neighbourhood, g_s (spatial filter) and g_r (range filter) plays a vital role in smoothing the image. The specification of these two filters determines the amount of filtering on an image. One must know that it is a crucial task to fix the value to g_s and g_r, because they determine the filtering quantity. For the testing images, g_s can be set to 2 and alter g_r, then g_r to 1 and alter g_s, whereas the size of the neighbourhood can be fixed as 5×5.

The proposed adaptive fusion method is compared with other foremost fusion methods including wavelet, curvelet and contourlet transformation domains using above fusion

Figure 3. **Original CT and MRI and their Corresponding Noisy Images Top Row: set-1 Bottom Row: Set-2.**

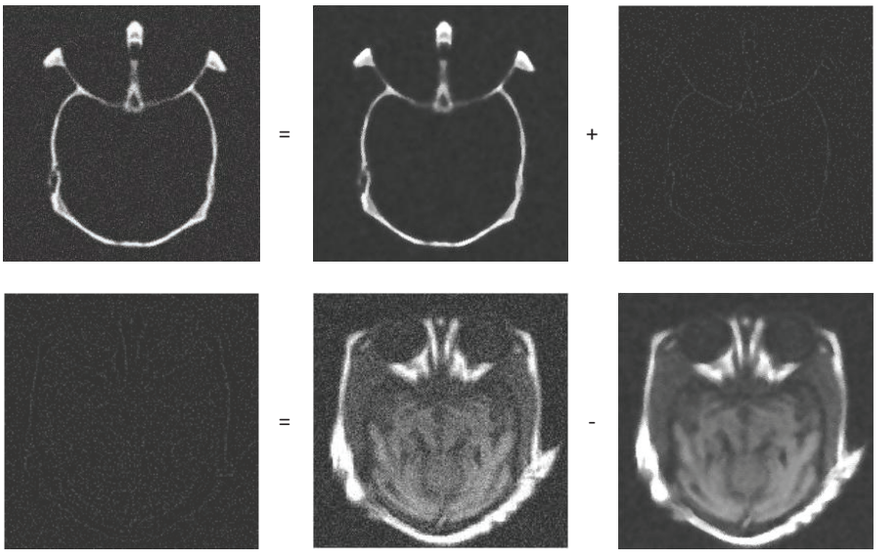

Figure 4. **Models for Noisy and Residual Top : Noise = Denoise + Residual Down : Residual = Noise + Denoise.**

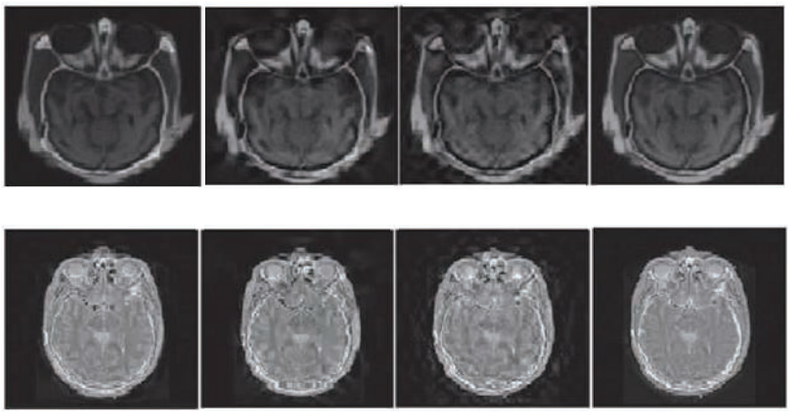

Table 1. **Comparison Result for Fusion of CT&MRI Noisy Images (set 1)**

	Entropy	Q^{F}_{AB}	*Standard Deviation*	*Fusion Symmetry*	*VIF*	*MI*
DWT	6.0127	0.6102	31.8652	0.2469	0.6145	2.1675
CT	6.2256	0.5175	32.5237	0.2472	0.6374	2.1862
NSCT	5.8962	0.6750	32.4631	0.2540	0.6281	2.1840
Proposed	6.2954	0.6830	32.5988	0.2498	0.6872	2.1868

Table 2. **Comparison Result for Fusion of CT&MRI Images (set 2)**

	Entropy	Q^{F}_{AB}	*Standard Deviation*	*Fusion Symmetry*	*VIF*	*MI*
DWT	5.1986	0.5170	59.7129	0.0386	0.5733	2.0478
CT	5.5788	0.3968	60.4159	0.0226	0.5749	2.0723
NSCT	5.4370	0.5626	60.2674	0.0375	0.5872	2.0719
Proposed	5.5793	0.5758	60.8729	0.0328	0.5895	2.0825

assessment parameters. In the spatial domain, the average fusion has been performed after denoising both corrupted images by bilateral filter. In wavelet domain, DWT based fusion can be accomplished over the denoised images by wavelet threshold. Similarly, denoising and fusion have been conducted based on curvlet denoising and fusion in curvelet domain. Performance evaluation has been conducted for all fused images obtained by proposing and comparison methods. Results are located in table 1 and 2 for two different sets of medical images. It is very important notice that the large values of standard deviation, edge strength, entropy, VIF, fusion symmetry and MI denote high quality of fused images.

Table 1 shows the effectiveness of the proposed method by checking the level of denoise and fusion performance of the tested CT and MRI brain multimodality images shown in the first row of fig. 3. Both are captured from two different modalities, which provide different information naturally. CT images are better choice for bone and hard tissues at the same time MR images give more details about soft tissues. Obviously, merging two images add additional and complement information to the fused image. By checking entropy values in table 1, it is easily identified that the proposed approach contributes more details to the fused image from input images. Similarly, the high values of edge strength and standard deviation shows that the robustness of the proposed approach with respect to strong edges and more information in comparison with other methods like DWT, CT and NSCT in table-1. The low value of fusion symmetry indicates that the visual quality of the proposed method is better than curvelet and contourlet based fusion methods. The second set of images, shown in the second row of fig. 3, is very useful in brain analysis while it gives complementary details in its fused image and the visual presentation is shown in fig. 5. The image representation of the comparison methods such as Curvelet- based , wavelet-based and contourlet-based fusion is also given in fig 5. The parameters discussed previously are applied to the proposed method and comparison methods for image set 2. According to the tabular results, it is evaluated that the proposed method obtains higher values and is shown in table-2.

Conclusion

The proposed method applied the significant characteristics of the suggested bilateral, curvelet and 2D modulated filter bank for the fusion of multimodal medical noisy images. The resultant image is more powerful because, the multiscale curvelet oriented method pay much attention over the curvy details, bilateral based approach yields improved results about linear edges and smoothed regions and 2D modulated filter bank provides excellent achievement in texture details in order to transfer these most significant information to the fused image. This approach not only denoising the medical images but also dilutes the artifacts introduced by the curvelet based fusion method. Indeed, the quantitative assessment of the proposed method constitutes supreme than that of the approaches by wavelet, curvelet and contourlet transform based fusion methods.

References:

1. Jens, B. & Felix, N. (2008). Data Fusion. *Journal of ACM Computing Surveys*, 41(1), 1-40.
2. Shutao, Li., Haitao, Y. & Leyuan, F. (2012). *Groupsparse Representation with Dictionary Learning for Medical Image Denoising and Fusion*. IEEE Transactions on Biomedical Engineering, 59(12), 3450-3459.
3. Hall, D. L. & James, L. (1997). *An Introduction to Multisensor Data Fusion*. Proceedings of the IEEE, 85(1), 6-23.
4. Porter, B. C., Rubens, D. J., Strang, J. G., Smith, J., Totterman, S. & Parker, K. J. (2001). *Three-dimensional registration and fusion of ultrasound and MRI using major vessels as fiducial markers.* IEEE Transactions on Medical Imaging, 20(4), 354-359.
5. Toet, A. (1990). Hierarchical image fusion. *Journal of Machine Vision and Applications*, 3(1), 1-11.
6. Petrovic, V. S. & Xydeas, C. S. (2004). *Gradient-based Multi-resolution Image Fusion*. IEEE Transactions on Image Processing, 13(2), 228-237.
7. Gravel, P., Beaudoin, G. D. & Guise, J. A. (2004). *A Method for Modeling Noise in Medical Images*. IEEE Transactions on Medical Imaging, 23(10), 21-32.
8. Rabbani, H., Nezafat, R. & Gazor, S. (2009). *Wavelet-domain Medical Image Denoising using Bivariate Laplacian Mixture Model.* IEEE Transactions on Biomedical Engineering, 56(12), 2826-2837.
9. Lin, J, W., Laine, A. F. & Bergmann, S. R. (2001). *Improving PET-based Physiological Quantification through Methods of Wavelet Denoising*. IEEE

Transactions on Biomedical Engineering, 48(2), 202-212.

10. Drapaca, C. S. (2009). *A Nonlinear Total Variation-based Denoising Method with Two Regularization Parameters*. IEEE Transactions on Biomedical Engineering, 56(3), 582-586.
11. Oster, J., Pietquin, O., Kraemer, M. & Felblinger, J. (2010). *Nonlinear Bayesian Filtering for Denoising of Electrocardiograms Acquired in a Magnetic Resonance Environment.* IEEE Transactions on Biomedical Engineering, 57(7), 1628-1638.
12. Dabov, K., Foi, A., Katkovnik, V. & Egiazarian, K. (2007). *Image Denoising by Sparse 3-D Transform-domain Collaborative Filtering*. IEEE Transactions Image Process, August, 16(8), 2080-2095.
13. Coup´e, P., Yger, P., Prima, S., Hellier, P., Kervrann, C. & Barillot, C. (2008). *An Optimized Blockwise Non-local means Denoising Filter for 3-D Magnetic Resonance Images*. IEEE Transactions on Medical Imaging, 27(4), 425-441.
14. Bhadauria, H. S. & Dewal, M. L. (2013). Medical image denoising using adaptive fusion of curvelet transform and total variation. *Computers and Electrical Engineering*, 39(5), 1451-1460.
15. Angelini., E., Jin, D., Yinpeng, E., Peter, D., Heertum, V., Laine, R. L. & Andrew, F. (2004). *Fusion of Brushlet and Wavelet Denoising Methods for Nuclear Images*. 2nd IEEE International Symposium on Biomedical Imaging: Macro to Nano, April, 2, 1187-1191.
16. Paris, S., Kornprobst, P., Tumblin, J. & Durand, F.: 'Bilateral Filtering: Theory and Applications'. Foundations and Trends R in Computer Graphics and Vision., 4(1), 1-73.
17. Wen-Chung., K. & Ying-Ju, C. *Multistage Bilateral Noise Filtering and Edge Detection for Color Image Enhancement*. IEEE Transactions on Consumer Electronics, 51(4), 1346-1351.
18. Ali, F. E., El-Dokany, I. M., Saad, A. A. & El-Samie, F. E. (2010). A curvelet transform approach for the fusion of MR and CT images. *Journal of Modern Optics*, 57(4), 273-286.
19. Strack, J. L., Candes, E. J. & Donoho, D. L. (2000). *The Curvelet Transform for Image Denoising*. IEEE Transactions on Image Processing, 11(6), 670-684.
20. Shui, P. L. (2009). *Image Denoising using 2-D Separable Oversampled DFT Modulated Filter Banks*. IET Image Processing, 2009, 3(3), 163-173.
21. Tomasi, C. & Manduchi, R. (1998). *Bilateral Filtering for Gray and Color Images.* Proceedings of the 6th International Conference on Computer Vision, (pp. 839-846).
22. Candes, E. J. & Donoho, D. L. (2000). *Curvelets, Multi-resolution Representations, and Scaling Laws*. Proceedings of Wavelet Applications Signal Image Processing, 4419, pp. 1-12.
23. Bamberger, R. H. & Smith, M. J. T. (1992). *A Filter Bank for Directional Decomposition of Images: Theory and Design*. IEEE Transactions on Signal Process, 40(4), 882-893.
24. Nguyen, T. T. & Oraintara, S. (2005). *Multi-resolution Directional Filter Banks: Theory, Design, and Application*. IEEE Transactions on Signal Processing, 53(10), 3895-3905.
25. Singh, R. & Khare, A. Fusion of multimodal medical images using Daubechies complex wavelet transform – A multiresolution approach'. Information Fusion, http://dx.doi.org/10.1016/j.inffus.2012.09.005.
26. Mumford, D. & Shah, J. (1989). 'Optimal approximations by piecewise smooth functions and associated variational problems'. Comm.Pure Appl. Math., 1989, 42(5), 577-685.
27. Qu, G., Zhang, D. & Yan, P. (2002). Information measure for performance of image fusion. *Electronic Letters*, 38(7), 313-315.
28. Sheikh, H. R. & Bovik, A. C. (2006). *Image Information and Visual Quality*. IEEE Transactions on Image Processing, 15(2), 430-444.
29. Shutao, L., Bin, Y. & Jianwen, H. (2011). Performance comparison of different multi-resolution transforms for image fusion. *Information Fusion*, 12(2), 74-84.